

Scattering of a surface plasmon from a square-wave grating: A study using coupled mode theory

A. J. Chaves^{1,2} and N. M. R. Peres^{2,3}

¹ *Department of Physics, Instituto Tecnológico de Aeronáutica, DCTA, 12228-900 São José dos Campos, Brazil*

² *Department and Centre of Physics, and QuantaLab, University of Minho, Campus of Gualtar, 4710-057, Braga, Portugal and*

³ *International Iberian Nanotechnology Laboratory (INL), Av. Mestre José Veiga, 4715-330 Braga, Portugal*

We use coupled-mode theory to describe the scattering of a surface-plasmon polariton (SPP) from a square wave grating (Bragg grating) of finite extension written on the surface of either a metal-dielectric interface or a dielectric-dielectric interface covered with a graphene sheet. We find analytical solutions for the reflectance and transmittance of SPP's when only two modes (forward and backscattered) are considered. We show that in both cases the reflectance spectrum presents stop-bands where the SPP is completely back-scattered if the grating is not too shallow. In addition, the reflectance coefficient shows Fabry-Pérot oscillations when the frequency of the SPP is out the stop-band region. For a single dielectric well, we show that there are frequencies of transmission equal to 1. We show that the same physics occurs with graphene SPP's with the appropriate changes in the formalism.

I. INTRODUCTION

In a recent paper¹ coupled-mode theory² was used for describing a set of experimental results showing unidirectional reflectionless in parity-time metamaterial at optical frequencies (see also Ref. [3]). The metamaterial was itself made of a periodic arrangement of metallic nanostructures in an optical fiber. To our best knowledge, coupled-mode theory was first discussed by Yariv in the context of coupled waveguides⁴.

Coupled mode theory was quite popular in the seventies and the eighties of the last century. However, with the advent of powerful numerical methods its use has declined. The paper of Feng *et al.*¹ gives a nice example where coupled-mode theory allows an analytical analysis of a scattering experiment with the obvious insight that an analytical solution provides over a fully numerical one.

In the context of guided wave optics Taylor and Yariv provided⁵ a detailed analysis of co- and contra-directional coupling, which corresponds to forward- and back-scattering of a single propagating mode induced by a periodic perturbation. Such perturbation can be in the form of change of the dielectric function along the propagation direction or in the form of a Bragg grating imposed on the surface of the waveguide. The theory of electromagnetic propagation in periodic stratified media was first discussed by in great detail by Yeh, Yariv, and Hong⁶. In the context of the theory of lasers, a comparison between the transfer matrix method and coupled-mode theory was given by Makino⁷. Recently, coupled-mode theory was used for analysing the scattering of a electromagnetic modes in a waveguide with corrugated boundaries⁸.

In this work we discuss the application of coupled-mode theory to the back-scattering of a surface-plasmon polariton from a one-dimensional Bragg grating imposed on the surface of a metal-dielectric interface. As a second example, we consider a graphene sheet covering a finite

Bragg grating and also in this case the back-scattering of a graphene surface-plasmon polariton is discussed. To our best knowledge, coupled-mode theory has not been applied so far to discuss the scattering of SPP's. However, a recent work has used this approach to discuss the excitation of SPP in gratings by far-field coupling⁹. The coupling of a Gaussian laser beam to SPP in a metallic film using coupled-mode theory was discussed by Ruan *et al.*¹⁰. In the context of graphene physics, coupled-mode theory was recently used to discuss the excitation of localized plasmons of a graphene-based cavity with a Silver waveguide¹¹. Also, problems in the context of nonlinear optics can be treated using coupled-mode theory¹². Integrating numerically the coupled-mode equations, Petracek and Kuzmiak have described Anderson localization of channel SPP's in a disordered square-wave grating¹³. In a different context, Graczyk and Krawczyk have studied¹⁴ the propagation of magnetoelastic waves using the methods described in this article. The nonlinear interaction, promoted by a nonlinear second-order susceptibility tensor, between SPP's was considered first by Santamato and Maddalena¹⁵. Interesting enough, coupled-mode theory was adapted for describing coupling of Bose-Einstein condensates¹⁶. The same type of approach has been used for describing the field enhancement near plasmonic nanostructure under the effect of an external field¹⁷. The extension of the theory to chiral waveguides was achieved by Pelet and Engheta¹⁸, and constitutes a nice application of Lorentz's reciprocity theorem (see Appendix A).

Coupled-mode theory is able to output both numeric and analytical results. In this paper, our analytical results are approximated in the sense that only two modes, forward- and back-scattered modes, of the same frequency are considered. This is a good approximation, since in the wave-guide only two SPP modes exist (forward and backward propagating SPP modes). However we do neglect the possible emission of radiation when the

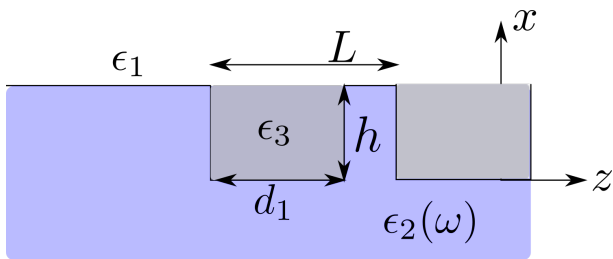


Figure 1. Unit cell of a dielectric grating. The bottom substrate has dielectric function $\epsilon_2(\omega) < 0$, the trench has dielectric function ϵ_3 , and the top dielectric has dielectric function ϵ_1 . Below we will consider $\epsilon_3 = \epsilon_1 = 1$. We assume that a surface-plasmon polariton is impinging from the left on the Bragg grating and is scattered from it. The reflectance coefficient, \mathcal{R} , is computed using coupled-mode theory.

SPP impinges on the grating. Indeed, in the context of scattering of graphene's SPP's by abrupt interfaces, it has been shown that the coupling of the SPP to the radiation modes is weak^{19,20}, and, therefore, the same is expected here. We note, however, that the formalism is general and there is no impediment to the inclusion of both radiative and evanescent modes in it. The price to pay may be the lack of an analytical solution.

The paper is organized as follows: In Sec. II we review the first steps of the derivation of coupled-mode equations, which are a reformulation of Maxwell's equations. In Sec. III we review the derivation of the orthogonality condition for bounded modes (radiation-modes orthogonality condition is not discussed). In Sec. IV we simplify the coupled-mode equations, expressing them in terms of forward and back-scattered amplitudes. In Sec. V we particularize coupled-mode equations to the case where only two degenerate modes in frequency are coupled and find a general solution using transfer-matrix method for a square-wave Bragg grating. In Sec. VI (Sec. VII) the scattering of metallic SPP's (graphene SPP's) from a Bragg grating is discussed. We conclude the paper with a brief discussion in Sec. VIII

II. DERIVATION OF THE COUPLED-MODE EQUATIONS: A REVIEW

For completeness (and presumably because this technique has fallen into oblivion), in this section we follow Marcuse's book²¹ in the derivation of coupled-mode equations (see also refs. [22–24, and 26]; we note here that there are many flavors of coupled-mode theories. For example in Yariv and Yeh²⁴ the paraxial approach is used). We choose a particular geometry for our system: a metal-dielectric interface, where a Bragg grating, extending over a finite region, is written on the surface of the metal (see Fig. 1). We consider a harmonic dependence for the fields of the form $e^{-i\omega t}$. Maxwell's equations in

space and time read

$$\nabla \times \mathbf{H} = \epsilon_0 \epsilon \frac{\partial \mathbf{E}}{\partial t}, \quad (1)$$

$$\nabla \times \mathbf{E} = -\mu_0 \frac{\partial \mathbf{H}}{\partial t}, \quad (2)$$

or, in frequency space,

$$\nabla \times \mathbf{H} = -i\omega \epsilon_0 \epsilon \mathbf{E}, \quad (3)$$

$$\nabla \times \mathbf{E} = i\omega \mu_0 \mathbf{H}. \quad (4)$$

Next we decompose the fields into their transverse and longitudinal components (we assume propagation along the z -direction for definiteness)

$$\mathbf{E} = \mathbf{E}_t + \mathbf{E}_z, \quad (5)$$

$$\mathbf{H} = \mathbf{H}_t + \mathbf{H}_z. \quad (6)$$

This decomposition will allow to identify the transverse modes of the unperturbed wave-guide. The differential operator is also decomposed in a similar way as

$$\nabla = \nabla_t + \mathbf{e}_z \frac{\partial}{\partial z}. \quad (7)$$

We can decompose the curl of a vector field \mathbf{A} in its transverse and longitudinal components as

$$(\nabla \times \mathbf{A})_t = \nabla_t \times \mathbf{A}_z + \mathbf{e}_z \times \frac{\partial \mathbf{A}_t}{\partial z}, \quad (8)$$

$$(\nabla \times \mathbf{A})_z = \nabla_t \times \mathbf{A}_t, \quad (9)$$

which follows from the identity

$$\left(\nabla_t + \mathbf{e}_z \frac{\partial}{\partial z} \right) \times (\mathbf{A}_t + \mathbf{A}_z) = \nabla_t \times \mathbf{A}_t + \nabla_t \times \mathbf{A}_z + \mathbf{e}_z \times \frac{\partial \mathbf{A}_t}{\partial z}. \quad (10)$$

Using this decomposition, Maxwell's equations imply that

$$\mathbf{E}_z = \frac{i}{\omega \epsilon_0 \epsilon} \nabla_t \times \mathbf{H}_t, \quad (11)$$

$$\mathbf{H}_z = -\frac{i}{\omega \mu_0} \nabla_t \times \mathbf{E}_t. \quad (12)$$

Therefore, knowing the transverse fields, the longitudinal components follow from the previous two equations. The equations for the transverse fields follow from combining Maxwell's equations with the previous two relations as

$$-\frac{i}{\omega \mu_0} \nabla_t \times (\nabla_t \times \mathbf{E}_t) + \mathbf{e}_z \times \frac{\partial \mathbf{H}_t}{\partial z} = -i\omega \epsilon_0 \epsilon \mathbf{E}_t, \quad (13)$$

and

$$\frac{i}{\omega \epsilon_0} \nabla_t \times \left(\frac{1}{\epsilon} \nabla_t \times \mathbf{H}_t \right) + \mathbf{e}_z \times \frac{\partial \mathbf{E}_t}{\partial z} = i\omega \mu_0 \mathbf{H}_t. \quad (14)$$

Equations (13) and (14) are in general hard to solve. However, for the system considered in our problem (see Fig. 1), a simple analytical solution to the transverse modes exists in the form of evanescent waves in the direction perpendicular to propagation of the SPP.

A. Modes of the ideal (non-perturbed) waveguide

We now assume that the propagation along the z -direction of the transverse modes (without the grating, that is, there is translation symmetry along z) has the form $e^{i\beta z}$, corresponding to a right-propagating mode. This simplifies the derivative in order to the z -coordinate, leading to

$$\frac{1}{\omega\mu_0}\nabla_t \times (\nabla_t \times \mathcal{E}_t) - \beta \mathbf{e}_z \times \mathcal{H}_t = \omega\epsilon_0 \mathcal{E}_t, \quad (15)$$

$$\frac{1}{\omega\epsilon_0}\nabla_t \times \left(\frac{1}{\epsilon} \nabla_t \times \mathcal{H}_t \right) + \beta \mathbf{e}_z \times \mathcal{E}_t = \omega\mu_0 \mathcal{H}_t, \quad (16)$$

where \mathcal{E}_t and \mathcal{H}_t are the transverse electric and magnetic fields of the mode, respectively. Note that here \mathcal{E}_t and \mathcal{H}_t do not depend on z . The longitudinal components follow from Eqs. (11) and (12) with the electric and magnetic fields replaced by the transverse mode components. We shall assume when computing the modes that they are a function of the coordinate x alone (translation symmetry along the y -direction and propagation along the z -direction only). Furthermore, we consider the TM case only, where the electric field has x and z components and the magnetic field has only a finite y component. This particular choice is characteristic of a SPP field. All this implies that

$$\nabla_t \times \mathcal{E}_t = 0, \quad (17)$$

and

$$\mathbf{e}_z \times \mathcal{H}_t = -\mathbf{e}_x \mathcal{H}_y(x), \quad (18)$$

Therefore, it follows from Eq. (15) that

$$\mathcal{E}_x(x) = \frac{\beta}{\omega\epsilon_0\epsilon(x)} \mathcal{H}_y(x). \quad (19)$$

On the other hand, we have

$$\nabla_t \times \mathcal{H}_t = \mathbf{e}_z \frac{\partial \mathcal{H}_y(x)}{\partial x}, \quad (20)$$

and

$$\nabla_t \times (\epsilon^{-1}(x) \nabla_t \times \mathcal{H}_t) = -\mathbf{e}_y \frac{\partial}{\partial x} \left(\frac{1}{\epsilon(x)} \frac{\partial \mathcal{H}_y(x)}{\partial x} \right), \quad (21)$$

and

$$\mathbf{e}_z \times \mathcal{E}_t = \mathbf{e}_y \mathcal{E}_x(x). \quad (22)$$

from where, together with Eq. (16), it follows that

$$-\frac{1}{\omega\epsilon_0} \frac{\partial}{\partial x} \left(\frac{1}{\epsilon(x)} \frac{\partial \mathcal{H}_y(x)}{\partial x} \right) + \frac{\beta^2}{\omega\epsilon_0\epsilon(x)} \mathcal{H}_y(x) = \omega\mu_0 \mathcal{H}_y(x), \quad (23)$$

or

$$\epsilon(x) \frac{\partial}{\partial x} \left(\frac{1}{\epsilon(x)} \frac{\partial \mathcal{H}_y(x)}{\partial x} \right) + \omega^2 \mu_0 \epsilon_0 \epsilon(x) \mathcal{H}_y(x) - \beta^2 \mathcal{H}_y(x) = 0. \quad (24)$$

The z -component of the electric field reads

$$\mathcal{E}_z(x) = \frac{i}{\omega\epsilon_0\epsilon(x)} \frac{\partial \mathcal{H}_y(x)}{\partial x}, \quad (25)$$

from Eq. (11). Equations (19), (24), and (25) are all we need to solve the problem of a rectangular wave-guide, extending to infinity along the y -direction (translation symmetry) and with propagation along the z -direction only, and showing confinement along the x -direction, due to the dependence of $\epsilon(x)$ on x .

B. Expanding the fields in the modes and the coupled-mode equations

Once the transverse modes are obtained, a general transverse field (including the case where the dielectric function depends on z) can be written as a superposition of those modes:

$$\mathbf{E}_t = \sum_{\nu=1}^N a_{\nu} \mathcal{E}_{\nu,t} + \sum_{j=1}^M \int_0^{\infty} a_{\rho,j} \mathcal{E}_{\rho,j,t} d\rho, \quad (26)$$

$$\mathbf{H}_t = \sum_{\nu=1}^N b_{\nu} \mathcal{H}_{\nu,t} + \sum_{j=1}^M \int_0^{\infty} b_{\rho,j} \mathcal{H}_{\rho,j,t} d\rho, \quad (27)$$

that is, we assume that $\{\mathcal{E}_{\nu,t}, \mathcal{H}_{\nu,t}, \mathcal{E}_{\rho,j,t}, \mathcal{H}_{\rho,j,t}\}$ forms a complete basis. This is not always true. However, it has been shown²⁵ that the coupled-mode theory can be obtained from a variational principle. Therefore, the resulting equations in this section can be seen as the optimal description for a given incomplete basis.

In the previous two equations a_{ν}/b_{ν} refer to the guided modes, whereas $a_{\rho,j}/b_{\rho,j}$ refer to the continuum of states (propagating and evanescent modes), and are in general a function of z . For simplifying the notation, we write simply

$$\mathbf{E}_t = \sum_{\nu} a_{\nu}(z) \mathcal{E}_{\nu,t}, \quad (28)$$

$$\mathbf{H}_t = \sum_{\nu} b_{\nu}(z) \mathcal{H}_{\nu,t}, \quad (29)$$

where the sum over ν has implicit a summation and an integration over both discrete and continuous modes, respectively. The coefficients of the expansion are now a function of z since we are considering a more general dielectric function: $\epsilon(x, z)$. The modes, however, are z -independent. Next we introduce these expansions in Eqs. (13) and (14). From Eq. (13) it follows that

$$\mathbf{e}_z \times \frac{\partial}{\partial z} \left(\sum_{\nu} b_{\nu}(z) \mathcal{H}_{\nu,t} \right) = -i\omega\epsilon_0\epsilon(x, z) \sum_{\nu} a_{\nu}(z) \mathcal{E}_{\nu,t}, \quad (30)$$

or

$$-\sum_{\nu} b'_{\nu}(z) \mathcal{H}_{\nu,y} = -i\omega\epsilon_0\epsilon(x, z) \sum_{\nu} a_{\nu}(z) \mathcal{E}_{\nu,x}, \quad (31)$$

where $b'(z)$ stands for the derivative of $b_\nu(z)$ in order to z . In the case where $\epsilon(x, z) = \epsilon(x)$ the modes satisfy equation (19):

$$-i\beta_\nu \mathcal{H}_{\nu,y} = -i\omega\epsilon_0\epsilon(x)\mathcal{E}_{\nu,x}. \quad (32)$$

Multiplying the previous equation by $a_\nu(z)$, summing over ν , and adding the result to Eq. (31) it follows that

$$\sum_\nu [b'_\nu(z) - i\beta_\nu a_\nu(z)]\mathcal{H}_{\nu,y} - i\omega\epsilon_0[\epsilon(x, z) - \epsilon(x)] \sum_\nu a_\nu(z)\mathcal{E}_{\nu,x} = 0. \quad (33)$$

From Eq. (14), it follows

$$-\frac{i}{\omega\epsilon_0} \sum_\nu b_\nu(z) \frac{\partial}{\partial x} \left(\frac{1}{\epsilon(x, z)} \frac{\partial \mathcal{H}_{\nu,y}(x)}{\partial x} \right) + \sum_\nu a'_\nu(z)\mathcal{E}_{\nu,x} = i\omega\mu_0 \sum_\nu b_\nu(z)\mathcal{H}_{\nu,y}. \quad (34)$$

In the case where $\epsilon(x, z) = \epsilon(x)$ the modes satisfy equation (24):

$$-\frac{i}{\omega\epsilon_0} \frac{\partial}{\partial x} \left(\frac{1}{\epsilon(x)} \frac{\partial \mathcal{H}_{\nu,y}(x)}{\partial x} \right) + i\beta_\nu \mathcal{E}_{\nu,x} = i\omega\mu_0 \mathcal{H}_{\nu,y}. \quad (35)$$

Using this result in the previous equation and after proceeding as before in the derivation of Eq. (33), it follows

$$-\frac{i}{\omega\epsilon_0} \sum_\nu b_\nu(z) \frac{\partial}{\partial x} \left[\left(\frac{1}{\epsilon(x, z)} - \frac{1}{\epsilon(x)} \right) \frac{\partial \mathcal{H}_{\nu,y}(x)}{\partial x} \right] + \sum_\nu [a'_\nu(z) - i\beta_\nu b_\nu(z)] \mathcal{E}_{\nu,x} = 0. \quad (36)$$

Equations (33) and (36) are the starting point for the derivation of the differential equations for the amplitudes $a_\nu(z)$ and $b_\nu(z)$.

III. ORTHOGONALITY RELATION AND NORMALIZATION CONDITION

In this section we derive the orthogonality and normalization conditions. It is useful if the reader goes over the Appendix A first, where Lorentz reciprocity theorem is derived.

A. Orthogonality relation

A detailed derivation of the orthogonality condition is given Appendix B and reads:

$$(\beta_\mu - \beta_\nu) \int dx (\mathcal{E}_{\nu,t} \times \mathcal{H}_{\mu,t}^* - \mathcal{E}_{\mu,t}^* \times \mathcal{H}_{\nu,t}) \cdot \mathbf{e}_z = 0, \quad (37)$$

where $\beta_\nu \neq \beta_\mu$, that is, the two modes are orthogonal in the sense of the previous integral, where we assumed that the system is lossless (ϵ real). The previous orthogonality relation can be simplified if we apply Eq. (B6) to a backwards traveling mode, that is, with a propagation

phase $e^{-i\beta_\nu z}$. Assuming that the mode ν is changed to a backwards propagating mode, this leads to

$$(\beta_\mu + \beta_{\bar{\nu}}) \int dx (\mathcal{E}_{\bar{\nu},t} \times \mathcal{H}_{\mu,t}^* - \mathcal{E}_{\mu,t}^* \times \mathcal{H}_{\bar{\nu},t}) \cdot \mathbf{e}_z = 0, \quad (38)$$

where $\bar{\nu}$ refers to the backwards traveling mode. This mode relates to the the forward propagating mode as follows: $\mathbf{E}_{\bar{\nu},t} = \mathbf{E}_{\nu,t}$ and $\mathbf{H}_{\bar{\nu},t} = -\mathbf{H}_{\nu,t}$ (and $\beta_{\bar{\nu}} = -\beta_\nu$), which implies that Eq. (38) can be written, for $\beta_\nu \neq \beta_\mu$, as

$$(\beta_\mu - \beta_\nu) \int dx (\mathcal{E}_{\nu,t} \times \mathcal{H}_{\mu,t}^* + \mathcal{E}_{\mu,t}^* \times \mathcal{H}_{\nu,t}) \cdot \mathbf{e}_z = 0, \quad (39)$$

and adding Eqs. (37) and (39) it follows that

$$\int dx \mathcal{E}_{\nu,t} \times \mathcal{H}_{\mu,t}^* \cdot \mathbf{e}_z = 0, \quad \beta_\nu \neq \beta_\mu. \quad (40)$$

We note that the expression (40) does not apply if $\beta_\mu = \beta_\nu$, since in this case we have $(\beta_\mu + \beta_{\bar{\nu}} = 0)$ in Eq. (38). For the particular case of the system we are considering, we have

$$\mathcal{E}_{\nu,t} \times \mathcal{H}_{\mu,t}^* = -\mathbf{e}_x \mathcal{E}_{\nu,z} \mathcal{H}_{\mu,y}^* + \mathbf{e}_z \mathcal{E}_{\nu,x} \mathcal{H}_{\mu,y}^*, \quad (41)$$

therefore the orthogonalization condition reads

$$\int dx \mathcal{E}_{\nu,x} \mathcal{H}_{\mu,y}^* = 0. \quad (42)$$

For forward scattered and backscattered modes with the same absolute value of β we have to use relation (37) instead.

B. Normalization condition

Having derived the orthogonality condition (40), we need to impose the normalization condition on the modes. The time averaged Poynting vector along the z -direction reads

$$S_{\nu,z} = \frac{1}{2} \Re(\mathcal{E}_\nu \times \mathcal{H}_\nu^*) \cdot \mathbf{e}_z, \quad (43)$$

which corresponds to the power transported per unit area by the mode ν along the z -direction. Therefore, the power \mathcal{P} per unit length transported along the z -direction reads

$$\mathcal{P} = \frac{1}{2} \int dx \Re(\mathcal{E}_\nu \times \mathcal{H}_\nu^*) \cdot \mathbf{e}_z = \frac{\beta}{2\omega\epsilon_0} \int dx \frac{1}{\epsilon(x)} \mathcal{H}_{\nu,y} \mathcal{H}_{\nu,y}^*, \quad (44)$$

where we have assumed a real $\epsilon(x)$. Therefore, we choose the normalization of the normal modes as

$$\int dx \frac{1}{\epsilon(x)} \mathcal{H}_{\nu,y} \mathcal{H}_{\nu,y}^* = \mathcal{P} \frac{2\omega\epsilon_0}{|\beta|}. \quad (45)$$

Typically, \mathcal{P} is chosen as 1 W/m^2 . The absolute value of $|\beta|$ ensures that the RHS of Eq. (45) is positive, as is the LHS. Note that the previous equation holds only for modes whose integral over the full range of x is finite. In particular, the previous equation does not apply to the radiative modes, as these are not normalizable in the sense of Eq. (45). Since in the problems we consider below we do not take radiative modes into account, we will not discuss how to modify equation (45) for accommodating these modes in the normalization condition (see, however, Ref. [27]).

IV. SIMPLIFICATION OF THE DIFFERENTIAL EQUATIONS FOR THE AMPLITUDES

In this section we aim at simplifying the coupled mode equations derived before. Let us now go back to Eqs. (33) and (36). We multiply Eq. (33) by $\mathcal{E}_{\mu,x}^*$:

$$\sum_{\nu} [b'_{\nu}(z) - i\beta_{\nu} a_{\nu}(z)] \mathcal{E}_{\mu,x}^* \mathcal{H}_{\nu,y} - i\omega\epsilon_0 [\epsilon(x,z) - \epsilon(x)] \sum_{\nu} a_{\nu}(z) \mathcal{E}_{\mu,x}^* \mathcal{E}_{\nu,x} = 0. \quad (46)$$

Integrating the previous equation over the transverse coordinate x and using the orthogonalization condition we obtain

$$b'_{\mu}(z) - i\beta_{\mu} a_{\mu}(z) = \frac{i\omega\epsilon_0}{2\mathcal{P}} \sum_{\nu} a_{\nu}(z) \int dx [\epsilon(x,z) - \epsilon(x)] \mathcal{E}_{\mu,x}^* \mathcal{E}_{\nu,x}. \quad (47)$$

We now multiply Eq. (36) by $\mathcal{H}_{\mu,y}^*$

$$- \frac{i}{\omega\epsilon_0} \sum_{\nu} b_{\nu}(z) \mathcal{H}_{\mu,y}^* \frac{\partial}{\partial x} \left[\left(\frac{1}{\epsilon(x,z)} - \frac{1}{\epsilon(x)} \right) \frac{\partial \mathcal{H}_{\nu,y}}{\partial x} \right] + \sum_{\nu} [a'_{\nu}(z) - i\beta_{\nu} b_{\nu}(z)] \mathcal{H}_{\mu,y}^* \mathcal{E}_{\nu,x} = 0. \quad (48)$$

Integrating the previous equation over the transverse coordinate x and using the orthogonalization condition we obtain

$$a'_{\mu}(z) - i\beta_{\mu} b_{\mu}(z) = \frac{i}{2\mathcal{P}\omega\epsilon_0} \sum_{\nu} b_{\nu}(z) \int dx \mathcal{H}_{\mu,y}^* \times \frac{\partial}{\partial x} \left[\left(\frac{1}{\epsilon(x,z)} - \frac{1}{\epsilon(x)} \right) \frac{\partial \mathcal{H}_{\nu,y}}{\partial x} \right]. \quad (49)$$

Next we recall that

$$\mathcal{E}_z(x) = \frac{i}{\omega\epsilon_0\epsilon(x)} \frac{\partial \mathcal{H}_y(x)}{\partial x}. \quad (50)$$

These two last results allows to write the identity

$$\int dx \mathcal{H}_{\mu,y}^* \frac{\partial}{\partial x} \left[\left(\frac{1}{\epsilon(x,z)} - \frac{1}{\epsilon(x)} \right) \frac{\partial \mathcal{H}_{\nu,y}}{\partial x} \right] = (\omega\epsilon_0)^2 \int dx \frac{\epsilon(x)}{\epsilon(x,z)} (\epsilon(x,z) - \epsilon(x)) \mathcal{E}_{\mu,z}^* \mathcal{E}_{\nu,z}, \quad (51)$$

obtained after an integration by parts. Thus,

$$a'_{\mu}(z) - i\beta_{\mu} b_{\mu}(z) = \frac{i\omega\epsilon_0}{2\mathcal{P}} \sum_{\nu} b_{\nu}(z) \int dx \frac{\epsilon(x)}{\epsilon(x,z)} (\epsilon(x,z) - \epsilon(x)) \mathcal{E}_{\mu,z}^* \mathcal{E}_{\nu,z}. \quad (52)$$

We now introduce the quantities

$$K_{\mu,\nu}(z) = \frac{i\omega\epsilon_0}{4\mathcal{P}} \int dx [\epsilon(x,z) - \epsilon(x)] \mathcal{E}_{\mu,x}^* \mathcal{E}_{\nu,x}, \quad (53)$$

$$k_{\mu,\nu}(z) = \frac{i\omega\epsilon_0}{4\mathcal{P}} \int dx \frac{\epsilon(x)}{\epsilon(x,z)} (\epsilon(x,z) - \epsilon(x)) \mathcal{E}_{\mu,z}^* \mathcal{E}_{\nu,z}. \quad (54)$$

These last two equations allow us to write the differential equations for amplitudes a_{μ} and b_{μ} as

$$b'_{\mu}(z) - i\beta_{\mu} a_{\mu}(z) = 2 \sum_{\nu} a_{\nu}(z) K_{\mu,\nu}(z), \quad (55)$$

$$a'_{\mu}(z) - i\beta_{\mu} b_{\mu}(z) = 2 \sum_{\nu} b_{\nu}(z) k_{\mu,\nu}(z). \quad (56)$$

When the coupling constants are zero, we have

$$b'_{\mu}(z) - i\beta_{\mu} a_{\mu}(z) = 0, \quad (57)$$

$$a'_{\mu}(z) - i\beta_{\mu} b_{\mu}(z) = 0. \quad (58)$$

The solution of these two differential equations follows from taking the derivative of the first equation and using the second one, which leads to

$$b''_{\mu}(z) + \beta_{\mu}^2 b_{\mu}(z) = 0, \quad (59)$$

whose general solution is

$$b_{\mu}(z) = b_{\mu}^+ e^{i\beta_{\mu} z} - b_{\mu}^- e^{-i\beta_{\mu} z}, \quad (60)$$

and therefore

$$a_{\mu}(z) = b_{\mu}^+ e^{i\beta_{\mu} z} + b_{\mu}^- e^{-i\beta_{\mu} z}, \quad (61)$$

in order to satisfy the first order differential equation. Note that the minus sign in front of the coefficient b_{μ}^- is not arbitrary, as it encodes the symmetry: $\mathbf{E}_{\bar{\nu},t} = \mathbf{E}_{\nu,t}$, $\mathbf{H}_{\bar{\nu},t} = -\mathbf{H}_{\nu,t}$, when $\beta_{\bar{\nu}} = -\beta_{\nu}$. Also, the two different sub-indexes, μ and $\bar{\mu}$, remember us that $b_{\bar{\mu}}^-$ is the backscattered wave, and therefore it corresponds to another mode, that is degenerated in frequency with the mode b_{μ}^+ . These two solutions suggest we introduce, in the general case where the coupling constants are finite, the functions

$$b_{\mu}(z) = b_{\mu}^+(z) - b_{\bar{\mu}}^-(z), \quad (62)$$

and therefore

$$a_{\mu}(z) = b_{\mu}^+(z) + b_{\bar{\mu}}^-(z), \quad (63)$$

where $b^+(z)$ and $b^-(z)$ refer to forward and backwards propagating modes, respectively. We replace Eqs. (62) and (63) in Eqs. (55) and (56), leading to

$$\frac{db_{\mu}^+}{dz} - \frac{db_{\mu}^-}{dz} - i\beta_{\mu} (b_{\mu}^+ + b_{\mu}^-) = 2 \sum_{\nu} (b_{\nu}^+ + b_{\nu}^-) K_{\mu,\nu}(z), \quad (64)$$

$$\frac{db_{\mu}^+}{dz} + \frac{db_{\mu}^-}{dz} - i\beta_{\mu} (b_{\mu}^+ - b_{\mu}^-) = 2 \sum_{\nu} (b_{\nu}^+ - b_{\nu}^-) k_{\mu,\nu}(z). \quad (65)$$

Adding Eqs. (64) and (65) we obtain

$$\frac{db_{\mu}^{+}}{dz} - i\beta_{\mu}b_{\mu}^{+} = \sum_{\nu} K_{\mu,\nu}^{++}b_{\nu}^{+} + K_{\mu,\nu}^{+-}b_{\nu}^{-}. \quad (66)$$

Subtracting (64) from (65)

$$\frac{db_{\mu}^{-}}{dz} + i\beta_{\mu}b_{\mu}^{-} = \sum_{\nu} K_{\mu,\nu}^{-+}b_{\nu}^{+} + K_{\mu,\nu}^{--}b_{\nu}^{-}, \quad (67)$$

where

$$K_{\mu,\nu}^{s_1s_2} = s_1K_{\mu,\nu}(z) + s_2k_{\mu,\nu}(z), \quad (68)$$

where $s_1, s_2 = \pm 1$. The coefficients b_{μ}^{+} and b_{μ}^{-} are rapidly varying functions of z .

V. SOLUTION FOR A SQUARE-WAVE BRAGG GRATING

For a Bragg grating described by alternating dielectrics where inside each dielectric slab the permittivity depends only on the transverse direction x , it can be obtained an exact solution when only two modes are involved, which is a situation appropriate to our case. Let us consider:

$$\epsilon(x, z) = \begin{cases} \tilde{\epsilon}(x), & \text{if } nL < z < d_1 + nL, \\ \epsilon(x), & \text{if } d_1 + nL < z < (n+1)L, \end{cases} \quad (69)$$

with n an integer. The Bragg lattice has N unit cells. In the lattice described by Eq. (69), the coefficient $K_{\mu\nu}^{pq}$ will be constant inside each slab. From now we will consider only two modes, the forward and back-scattered with label μ . We simplify the notation so $b_{\mu}^{+} \equiv X$ and $b_{\mu}^{-} \equiv Y$. We define $K_{\mu\mu}^{++} = -K_{\mu\mu}^{--} \equiv u$ and $K_{\mu\mu}^{+-} = -K_{\mu\mu}^{-+} = -v$ when $nL < z < d_1 + nL$. Therefore, Eqs. (66) and (67) can be written as:

$$X' - i\beta X = uX + vY, \quad (70)$$

$$Y' + i\beta Y = -vX - uY. \quad (71)$$

The transmission and reflection coefficients can be defined as usual:

$$\mathcal{R} = \left| \frac{Y(0)}{X(0)} \right|^2, \quad (72a)$$

$$\mathcal{T} = \left| \frac{X(NL)}{X(0)} \right|^2. \quad (72b)$$

Now we will solve Eqs. (70) and (71) for $0 < z < d_1$. From (71):

$$X = -\frac{Y' + (i\beta + u)Y}{v}, \quad (73)$$

that can be combined into a single equation for Y using (70):

$$Y'' + (v^2 + \beta^2 - 2i\beta u - u^2)Y = 0, \quad (74)$$

and defining:

$$g = \sqrt{v^2 + (\beta - iu)^2}, \quad (75)$$

the solution of (74) can be written as:

$$Y(z) = Y_+ e^{igz} + Y_- e^{-igz}, \quad (76)$$

with Y_+ and Y_- constants, and substituting back in Eq. (73) we obtain:

$$X(z) = -Y_+ \frac{ig + i\beta + u}{v} e^{igz} - Y_- \frac{-ig + i\beta + u}{v} e^{-igz}. \quad (77)$$

To obtain the transfer matrix of the propagation between $z = 0$ and $z = d_1$, we need to write the components $Y(z = d_1)$ and $X(z = d_1)$ as function of $Y(z = 0)$ and $X(z = 0)$. Therefore, using Eqs. (76) and (77) for $z = 0$ we obtain:

$$Y(0) = Y_+ + Y_- \quad (78a)$$

$$X(0) = h_+ Y_+ + h_- Y_-, \quad (78b)$$

where we defined $h_{\pm} = -\frac{\pm g + i\beta + u}{v}$. And for $z = d_1$:

$$Y(d_1) = Y_+ e^{igd_1} + Y_- e^{-igd_1}, \quad (79a)$$

$$X(d_1) = h_+ Y_+ e^{igd_1} + h_- Y_- e^{-igd_1}. \quad (79b)$$

From Eqs. (78) we have:

$$Y_+ = \frac{X(0) - h_- Y(0)}{h_+ - h_-}, \quad (80a)$$

$$Y_- = -\frac{X(0) - h_+ Y(0)}{h_+ - h_-}, \quad (80b)$$

now using Eqs. (80) in Eqs. (79) we obtain:

$$Y(d_1) = \frac{e^{igd_1} - e^{-igd_1}}{h_+ - h_-} X(0) - \frac{h_- e^{igd_1} - h_+ e^{-igd_1}}{h_+ - h_-} Y(0), \quad (81)$$

$$X(d_1) = \frac{h_+ e^{igd_1} - h_- e^{-igd_1}}{h_+ - h_-} X(0) + \frac{h_+ h_- - e^{igd_1} + e^{-igd_1}}{h_+ - h_-} Y(0), \quad (82)$$

and after some algebra:

$$X(d_1) = (\cos(gd_1) + i\Delta_1 \sin(gd_1)) X(0) + \Delta_2 \sin(gd_1) Y(0), \quad (83)$$

$$Y(d_1) = -\Delta_2 \sin(gd_1) X(0) + (\cos(gd_1) - i\Delta_1 \sin(gd_1)) Y(0), \quad (84)$$

where we have defined $\Delta_1 \equiv \frac{\beta - iu}{g}$ and $\Delta_2 \equiv \frac{v}{g}$, with $\Delta_1^2 + \Delta_2^2 = 1$. This defines the propagation along any unit cell from $z = nL$ to $z = d_1 + nL$. The propagation from $z = d_1 + nL$ to $z = (n+1)L$ is given from the solution of:

$$\begin{aligned} X' - i\beta X &= 0, \\ Y' + i\beta Y &= 0, \end{aligned} \quad (85)$$

where the coupling constants $K_{\mu,\mu}^{s_1,s_2}$ vanishes because of the dielectric function (69). Therefore, we have the trivial solution: $X(z) = X(d_1)e^{i\beta z}$ and $Y(z) = Y(d_1)e^{-i\beta z}$. The total transfer matrix of the propagation along an entire unit cell is:

$$M = \begin{pmatrix} e^{i\theta_2} & 0 \\ 0 & e^{-i\theta_2} \end{pmatrix} \begin{pmatrix} \cos \theta_1 + i\Delta_1 \sin \theta_1 & \Delta_2 \sin \theta_1 \\ -\Delta_2 \sin \theta_1 & \cos \theta_1 - i\Delta_1 \sin \theta_1 \end{pmatrix} \quad (86)$$

where we defined $\theta_1 \equiv gd_1$ and $\theta_2 \equiv \beta d_2$, such that the transfer matrix that relates the right and left propagating fields impinging on each face of a unit cell $[X((n+1)L), Y((n+1)L)]^T = M[X(nL), Y(nL)]^T$ is (the super-index T refers to the transpose operation):

$$M = \begin{pmatrix} e^{i\theta_2} (\cos \theta_1 + i\Delta_1 \sin \theta_1) & e^{i\theta_2} \Delta_2 \sin \theta_1 \\ -e^{-i\theta_2} \Delta_2 \sin \theta_1 & e^{-i\theta_2} (\cos \theta_1 - i\Delta_1 \sin \theta_1) \end{pmatrix}. \quad (87)$$

From the eigenvalues of the above matrix we can obtain the Bloch phase γ :

$$\cos \gamma = \cos \theta_1 \cos \theta_2 - \Delta_1 \sin \theta_1 \sin \theta_2, \quad (88)$$

and from the Chebyshev identity²⁹, we can obtain the transmission and reflection coefficients from the propagation along N unit cells:

$$T = \frac{\sin^2 \gamma}{\sin^2 \gamma + |\Delta_2|^2 |\sin \theta_1|^2 \sin^2 (N\gamma)}, \quad (89a)$$

$$R = \frac{|\Delta_2|^2 |\sin \theta_1|^2 \sin^2 [N\gamma]}{\sin^2 \gamma + |\Delta_2|^2 |\sin \theta_1|^2 \sin^2 (N\gamma)}. \quad (89b)$$

We, therefore, obtained analytical formulas for the propagation of two coupled modes. This formalism will be used in the next two sections to obtain the propagation properties of SPPs in metallic and graphene gratings.

VI. SPP SCATTERING FROM A METALLIC GRATING

In this section we consider the scattering of a SPP from a Brag grating whose unit cell is represented in Fig. 1. The dielectric function ϵ_1 is vacuum, the dielectric $\epsilon_2(\omega)$ represent the optical response of the metal below the plasma frequency, and ϵ_3 is another dielectric, in principle different from ϵ_1 and $\epsilon_2(\omega)$.

A. SPP fields and dispersion relation

Let us consider an interface between a metal and a dielectric. The relative dielectric function of the metal is in the spectral range where $\epsilon_2(\omega) < 0$ and that of the dielectric is ϵ_1 , assumed constant. The dispersion relation of a surface-plasmon polariton at metallic interface with a dielectric is given by²⁸

$$q = \frac{\omega}{c} \sqrt{\frac{\epsilon_1 \epsilon_2(\omega)}{\epsilon_1 + \epsilon_2(\omega)}}. \quad (90)$$

The field of the SPP has the form²⁸

$$\mathbf{E}_\alpha(\mathbf{r}, t) = (E_{\alpha,x} \mathbf{e}_x + E_{\alpha,z} \mathbf{e}_z) e^{-\kappa_\alpha |x|} e^{i(qz - \omega t)}, \quad (91)$$

$$\mathbf{B}(\mathbf{r}, t) = B_y \mathbf{e}_y e^{-\kappa_\alpha |x|} e^{i(qz - \omega t)}, \quad (92)$$

where $\alpha = 1, 2$ defines the medium where the field is located. Using Maxwell's equations, we obtain

$$E_{\alpha,x} = \frac{q}{\omega \epsilon_0 \epsilon_\alpha} H_y, \quad (93)$$

$$E_{\alpha,z} = -i \text{sgn}(z) \frac{\kappa_\alpha}{\omega \epsilon_0 \epsilon_\alpha} H_y, \quad (94)$$

$$\kappa_\alpha = \sqrt{q^2 - \epsilon_\alpha \omega^2 / c^2}. \quad (95)$$

We note that $E_{\alpha,x}$ and H_y are the transverse fields, whereas $E_{\alpha,z}$ is the longitudinal component. The usual boundary conditions for the fields at an interface, $E_{1,z} = E_{2,z}$ and $B_{1,y} = B_{2,y}$, lead to the dispersion (90). Note that ϵ_1 and ϵ_2 must have different signs for satisfying the first boundary condition. Therefore, an SPP mode only exists when its frequency is below the plasma frequency. Indeed, we can show from Eq. (90) that the frequency region for the existence of the SPP obeys the condition

$$\omega < \frac{\omega_p}{\sqrt{\epsilon_1 + 1}}, \quad (96)$$

where ω_p is the plasma frequency of the metal. The determination of the magnitude H_y follows from the normalization condition (45), which has the form

$$\int dx \frac{1}{\epsilon(x)} \mathcal{H}_y(x) \mathcal{H}_y^*(x) = \mathcal{P} \frac{2\omega \epsilon_0}{|q|}, \quad (97)$$

or, in the case of the SPP field,

$$\int_{-\infty}^0 dx \frac{1}{\epsilon_2} e^{2\kappa_2 x} H_y^2 + \int_0^\infty dx \frac{1}{\epsilon_1} e^{-2\kappa_1 x} H_y^2 = \mathcal{P} \frac{2\omega \epsilon_0}{|q|}, \quad (98)$$

which leads to

$$\Leftrightarrow H_y^2 = \mathcal{P} \frac{4\omega \epsilon_0}{|q|} \frac{\kappa_1 \kappa_2 \epsilon_1 \epsilon_2}{\kappa_1 \epsilon_1 + \kappa_2 \epsilon_2}. \quad (99)$$

We also note that a mode with $\beta = q$ and another mode with $\beta = -q$ are orthogonal in the sense of Eq. (37) but not in the sense of Eq. (42). This happens because the simplified version does not apply to this *degenerate* case, as discussed before. Indeed, in the first case we have

$$\int dx [E_{q,x} H_{-q,y}^* - E_{-q,x}^* H_{q,y}] = - \int dx [E_{q,x} H_{q,y}^* + E_{q,x}^* H_{q,y}], \quad (100)$$

and since $E_{q,x} \propto iH_{q,y}$, the integral vanishes because the integrand adds to zero, where we have used the fact that time reversed fields obey the same Maxwell's equations upon the transformations $\mathbf{E}(-t) \rightarrow \mathbf{E}(t)$ and $\mathbf{H}(-t) \rightarrow -\mathbf{H}(t)$.

B. Dielectric profile

The system upon which the SPP will scatter is a square dielectric grating of period $L = d_1 + d_2$. As function of x , the dielectric profile reads

$$\epsilon(x, z) = \begin{cases} \epsilon_3 & \text{for } nL < z < d_1 + nL \\ \epsilon_2(\omega) & \text{for } nL + d_1 < z < d_1 + d_2 + nL \end{cases} \quad (101)$$

$$K_{q,q}(z) = \begin{cases} i \frac{q\epsilon_1(\epsilon_3 - \epsilon_2)\kappa_1 \sinh(h\kappa_2) e^{-h\kappa_2}}{\epsilon_2(\epsilon_1\kappa_1 + \epsilon_2\kappa_2)} & \text{for } nL < z < d_1 + nL \\ 0 & \text{for } nL + d_1 < z < d_1 + d_2 + nL \end{cases}, \quad (102)$$

and

$$k_{q,q}(z) = \begin{cases} i \frac{(\epsilon_3 - \epsilon_2)\kappa_1 \kappa_2^2 \sinh(h\kappa_2) e^{-h\kappa_2}}{q(\epsilon_1\kappa_1 + \epsilon_2\kappa_2)} & \text{for } nL < z < d_1 + nL \\ 0 & \text{for } nL + d_1 < z < d_1 + d_2 + nL \end{cases}, \quad (103)$$

from where the coupling constant $K_{q,q}^{s_1 s_2}$ (68) follows; the constant h is the height of the dielectric well/barrier. We note that the coupling constants $K_{q,q}$ and $k_{q,q}$ are zero when $h \rightarrow 0$ or $\epsilon_3 \rightarrow \epsilon_2$, which corresponds to the perfect interface. Therefore, the reflectance coefficient \mathcal{R} is zero in these cases.

C. Results for a single barrier

We first consider the case of a single well of width d_1 and height h . The results for the reflectance coefficient are given in Fig. 2. In the first panel we see that, $\mathcal{R} \rightarrow 0$ when $h \rightarrow 0$, as discussed above. Also there are heights different from zero for which there is perfect transmission. A similar phenomenon occurs when electrons are scattered from a potential well. From the central panel of the same figure we see that $\mathcal{R} \rightarrow 0$ when $\omega \rightarrow 0$, which makes sense since in this case we have essentially free radiation of very large wavelength and, therefore, unable to see the dielectric well. As ω approaches $\omega_p/\sqrt{2}$ we have that $\mathcal{R} \rightarrow 1$. The last panel shows a study of \mathcal{R} as function of h and ω , showing that for $h > 0.08\lambda_0$ the reflectance becomes insensitive to further increases in the well height. The almost absence of oscillations of the reflectance comes from the fact that $g^2 < 0$ [see Eq. (75)] for the parameters used, so the fields inside the well are evanescent, as discussed in detail in the next subsection.

D. Results for a Bragg grating

For a Bragg grating, the transmission and reflection can be obtained from Eqs. (89a) and (89b), with the Bloch phase given by Eq. (88). The propagation inside the dielectric well is determined by the value of g^2 .

with $n = 0, 1, 2, \dots$. Once the dielectric profile is known, we can compute the coupling constants $K_{\mu,\nu}$ and $k_{\mu,\nu}$ using Eqs. (53) and (54). Since $\epsilon(x, z) = \epsilon(x, z + L)$, the coupling constants are also periodic. In this case, because the dielectric functions vary in a step-like manner, they can be computed analytically, reading

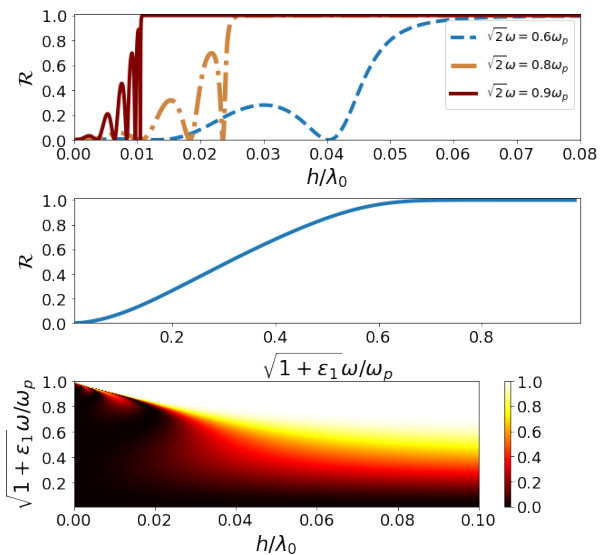


Figure 2. Reflectance coefficient. The plasma frequency was chosen equal to $\omega_p = 4$ eV. We take $\epsilon_3 = \epsilon_1 = 1$ and $d_1 = (1+1/4)\lambda_0$, with λ_0 the plasmon wavelength for the frequency $\omega_{spp} = 0.6\omega_p/\sqrt{2}$. In the top panel we show the reflectance as function of h . In the central panel $h = \lambda_0/2$. The bottom panel shows the reflectance as function of the frequency and h . The dielectric function of the metal is given by Drude formula $\epsilon_2(\omega) = 1 - \omega_p^2/\omega^2$.

For $g^2 > 0$ we have sinusoidal transmission while for $g^2 < 0$ we have evanescent transmission, with $g^2 = 0$ determining the crossing between those two regimes. When $\kappa_2 h \gg 1$ and $\epsilon_3 = \epsilon_1$ the function g^2 will always be negative, resulting in evanescent transport inside the dielectric well. In this section we will study the case when the dielectric 3 is also given by a metal with a corresponding

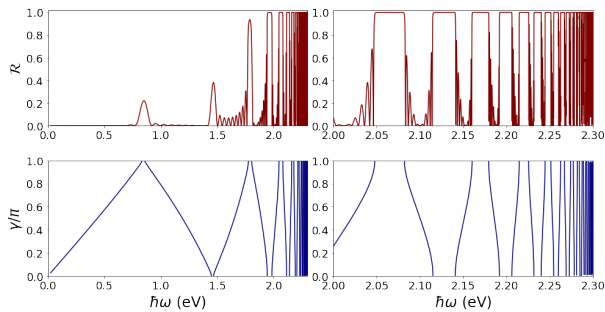


Figure 3. Top panels: Reflectance of a Bragg grating with $N = 10$. We have chosen λ_0 the plasmon wavelength for the energy of the SPP given by $\sqrt{2}\omega_{spp}/\omega_p = 0.6$, $\epsilon_1 = 1$, $\hbar\omega_p = 4$ eV, $d_1 = d_2 = h = \lambda_0/2$, $\epsilon_3 = 1 - \omega_p'^2/\omega^2$, and $\omega_p' = 2.3$ eV. The bottom panels are the dispersion relation as function of the Bloch phase $\gamma = kL$, with k the crystal wavenumber. The bandgaps coincide with the total reflection, as expected. Note the different horizontal scale in the left and right panels.

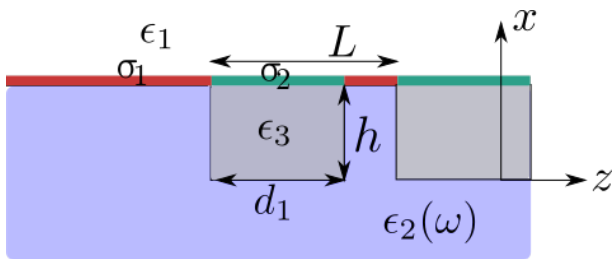


Figure 4. Unit cell of a dielectric grating for this section. It is the same system of Fig. 1 with the inclusion of alternating graphene strips with different conductivities σ_1 and σ_2 . Now we will consider that $\epsilon_2(\omega) > 0$ is constant.

dielectric constant $\epsilon_3 = 1 - \omega_p'^2/\omega^2$.

We show the results for the reflectance and dispersion relation in Fig. 3. We consider $\hbar\omega_p = 4$ eV and $\hbar\omega_p' = 2.3$ eV. The Bragg grating has $N = 10$, $L = \lambda_0$, $d_1 = d_2 = L/2$, where λ_0 is the wavelength of the plasmon (90) for a frequency of $0.4\omega_p$ and $\hbar\omega_p = 4$ eV. We have that $g^2 > 0$ for $\omega < \omega_p'$ and $g^2 \xrightarrow{\omega \rightarrow \omega_p'} \infty$. The divergence in g explains the large number of bands slightly below the energy of 2.3 eV in the bottom panel of Fig. 3. Note the correlation between the presence of stop-bands in the spectrum of the SPP and the value of 1 for the reflectance.

VII. SCATTERING OF GRAPHENE PLASMONS FROM A DIELECTRIC BRAGG GRATING

Now we consider a system with the geometry of Fig. 1 but with a graphene sheet on top with conductivity

σ_1 (σ_2) on top of the dielectric ϵ_2 (ϵ_3), as shown in Fig. 4. The presence of a graphene sheet corresponds to including a surface current in the Maxwell equation (3):

$$\nabla \times \mathbf{H} = \sigma \delta(x) \mathbf{E}_{\parallel} - i\omega \epsilon_0 \epsilon \mathbf{E}, \quad (104)$$

where σ is the 2D graphene conductivity and the sheet is located at the plane $x = 0$.

We consider, for simplicity, that the graphene conductivity is given by the Drude term²⁸:

$$\sigma_{\text{Drude}} = \frac{4i}{\pi} \frac{E_{F\alpha} \sigma_0}{\hbar\omega + i\Gamma_{\alpha}}, \quad (105)$$

with $\sigma_0 = e^2/(4\hbar)$, $E_{F\alpha}$ ($\alpha = 1, 2$) the Fermi energy in the graphene sheet relative to the Dirac Point, and Γ_{α}/\hbar is the relaxation rate. From now on we will consider $\Gamma_{\alpha} = 0$ as we are not interested in studying the effect of losses.

In this case, the boundary condition at the graphene interface leads to a different dispersion relation given by²⁸

$$\frac{\epsilon_1}{\kappa_1} + \frac{\epsilon_2}{\kappa_2} + i \frac{\sigma}{\epsilon_0 \omega} = 0, \quad (106)$$

whose solution in the electrostatic limit reads²⁸

$$q = \frac{\epsilon_1 + \epsilon_2}{4} \frac{(\hbar\omega)^2}{\alpha E_F \hbar c}, \quad (107)$$

where $\alpha \approx 1/137$ is the fine structure constant and E_F is the Fermi energy of doped graphene. We note that in addition to a modification of the dispersion relation, graphene plasmons exist as well defined excitation for energy scales smaller than the Fermi energy, and therefore in a different frequency range from that observed for noble metal plasmonics.

We can define a new dielectric tensor taking in account the graphene's conductivity:

$$\tilde{\epsilon}(x) = \epsilon + i\hat{\mathbf{r}} \frac{\sigma \delta(x)}{\omega \epsilon_0} \hat{\mathbf{r}}, \quad (108)$$

with $\hat{\mathbf{r}}$ the versor along the plane that contains the graphene sheet and therefore Eq. (104) becomes $\nabla \times \mathbf{H} = -i\omega \epsilon_0 \tilde{\epsilon}(x) \mathbf{E}$.

It can be easily show that the orthogonality relation and normalization conditions obtained in Sec. III do not change with a dielectric tensor given by Eq. (108). In this case, we can derive the coupled-mode equations when we have a more general graphene conductivity $\sigma(z)$ along the general dielectric function $\epsilon(x, z)$, obtaining again the same expression for Eqs. (66) and (66), with the new coefficients $K_{\mu, \nu}, k_{\mu, \nu}$ obtained in Appendix C:

$$K_{\mu,\nu}(z) = \frac{i\omega\epsilon_0}{4\mathcal{P}} \int dx [\epsilon(x,z) - \epsilon(x)] \mathcal{E}_{\mu,x}^* \mathcal{E}_{\nu,x}, \quad (109)$$

$$k_{\mu,\nu}(z) = -\frac{\sigma_1}{\sigma_2(z)} \frac{[\sigma_2(z) - \sigma_1]}{4\mathcal{P}} \mathcal{E}_{\mu,z}^*(0) \mathcal{E}_{\nu,z}(0) + \frac{i\omega\epsilon_0}{4\mathcal{P}} \int dx \frac{\epsilon(x)}{\epsilon(x,z)} (\epsilon(x,z) - \epsilon(x)) \mathcal{E}_{\mu,z}^* \mathcal{E}_{\nu,z}. \quad (110)$$

With the presence of a graphene sheet, the tangential magnetic field H_y is no longer continuous. Thus, we need to calculate the new normalization in the sense of Eq. (97), reading:

$$H_{2,y}^2 = \mathcal{P} \frac{4\omega\epsilon_0}{|q|} \frac{\kappa_1^3 \epsilon_2^2 \kappa_2}{\epsilon_1 \kappa_2^3 + \epsilon_2 \kappa_1^3}, \quad (111)$$

and the other components of the electromagnetic field can be calculated from:

$$H_{1,y} = -\frac{\kappa_2 \epsilon_1}{\kappa_1 \epsilon_2} H_{2,y}, \quad (112a)$$

$$E_{\alpha,z} = -i \frac{\kappa_\alpha \text{sgn}(x)}{\omega \epsilon_0 \epsilon_\alpha} H_{\alpha,y}, \quad (112b)$$

$$E_{\alpha,x} = \frac{q}{\omega \epsilon_0 \epsilon_\alpha} H_{\alpha,y}, \quad (112c)$$

with $\alpha = 1, 2$. Using Eqs. (111) and (112) in Eqs. (109) and (110) we obtain:

$$K_{q,q} = iq(\epsilon_3 - \epsilon_2) \frac{\kappa_1^3}{\epsilon_2 \kappa_1^3 + \epsilon_1 \kappa_2^3} \sinh(\kappa_2 h) e^{-\kappa_2 h}, \quad (113)$$

$$k_{q,q} = \frac{\sigma_1}{\sigma_2} \frac{\sigma_1 - \sigma_2}{\omega \epsilon_0 q} \frac{\kappa_1^3 \kappa_2^3}{\epsilon_2 \kappa_1^3 + \epsilon_1 \kappa_2^3} + i \frac{\epsilon_2}{\epsilon_3} (\epsilon_3 - \epsilon_2) \frac{\kappa_2^2 \kappa_1^3}{q(\epsilon_2 \kappa_1^3 + \epsilon_1 \kappa_2^3)} \sinh(\kappa_2 h) e^{-\kappa_2 h}, \quad (114)$$

where σ_α , with $\alpha = 1, 2$, is the Drude conductivity (105).

In the following we will show how the formalism works for two examples. First when $E_{F1} = E_{F2}$ and $\epsilon_2 \neq \epsilon_3$. Next we show the results for $E_{F1} \neq E_{F2}$ and $\epsilon_2 = \epsilon_3$.

1. Different substrates and same conductivity

First we show the results in Fig. 5 for a grating with $E_{F1} = E_{F2}$ and $\epsilon_3 = \epsilon_1 = 1$ and $\epsilon_2 = 2$. We can see that the bandwidths decreases as we increase the SPP frequency. In the electrostatic limit and $E_{F1} = E_{F2}$, we can simplify the coefficients $K_{q,q}, k_{q,q}$ to:

$$K_{q,q} \rightarrow iq \frac{\epsilon_3 - \epsilon_2}{\epsilon_2 + \epsilon_1} \frac{\zeta}{2}, \quad (115)$$

$$k_{q,q} \rightarrow iq \frac{\epsilon_2}{\epsilon_3} \frac{\epsilon_3 - \epsilon_2}{\epsilon_2 + \epsilon_1} \frac{\zeta}{2}, \quad (116)$$

with $\zeta = 2 \sinh(\kappa_2 h) e^{-\kappa_2 h}$ and $\zeta \rightarrow 1$ when $\kappa_2 h \gg 1$. In this case we have that the functions $K_{qq}^{++} = u$ and

$K_{qq}^{-+} = v$ are:

$$u = \zeta \frac{iq}{2} \frac{\epsilon_3^2 - \epsilon_2^2}{\epsilon_3(\epsilon_1 + \epsilon_2)}, \quad (117)$$

$$v = -\zeta \frac{iq}{2} \frac{(\epsilon_3 - \epsilon_2)^2}{\epsilon_3(\epsilon_1 + \epsilon_2)}, \quad (118)$$

and we can calculate g from Eq. (75):

$$g = q\sqrt{F(\epsilon_1, \epsilon_2, \epsilon_3, \zeta)}, \quad (119)$$

with:

$$F = \frac{(\epsilon_1 + (1 - \zeta)\epsilon_2 + \zeta\epsilon_3)((1 + \zeta)\epsilon_3\epsilon_2 + 2\epsilon_3\epsilon_1 - 2\zeta\epsilon_2^2)}{\epsilon_3(\epsilon_1 + \epsilon_2)^2}, \quad (120)$$

and so, the functions $\Delta_1 = (\beta - iu)/g$ and $\Delta_2 = v/g$ that appears inside the transfer matrix (87) are given by:

$$\Delta_1 = \frac{1}{2} \frac{2\epsilon_3(\epsilon_1 + \epsilon_2)\sqrt{F} + \zeta\epsilon_3^2 - \zeta\epsilon_2^2}{\epsilon_3(\epsilon_1 + \epsilon_2)\sqrt{F}}, \quad (121a)$$

$$\Delta_2 = -\zeta \frac{i}{2} \frac{(\epsilon_3 - \epsilon_2)^2}{\epsilon_3(\epsilon_1 + \epsilon_2)\sqrt{F}}, \quad (121b)$$

note that as ω (or q) increases, we have $\zeta \rightarrow 1$. If we ignore the dependence on frequency of the dielectrics constants, the functions Δ_1 and Δ_2 will become frequency independent and so the propagation properties, that are expressed in the transfer matrix approach by Eq. (89a), will only depend on the angles θ_1, θ_2 , both proportional to $q \propto \omega^2$. We show the periodic dependence of the reflection as function of q in Fig. 6. In the same figure the stop-band appears for $q = \frac{2\pi}{\lambda_0}(2j+1)$, with j an integer. As before, there is a correlation between the presence of stop-band and reflectance equal to 1.

2. Different conductivities and same substrate

Next we show in Fig. 7 the results for a grating of alternating strips of graphene with different Fermi energies deposited on the same substrate with dielectric constant ϵ_2 . For the widths, we used $d_1 = d_2 = \lambda_0/2$, where $\lambda_0 \approx 9 \mu\text{m}$ is the graphene plasmon wavelength obtained from Eq. (107) for $E_{F1} = 0.3 \text{ eV}$ and $\hbar\omega = E_{F1}/2$. We can see that the first stop-band appears centered in the frequency $\approx 0.27E_{F1}/\hbar$. Compared to the previous section, we did not impose the phase matching $\theta_1 = \theta_2$ condition. Therefore, there is no simple relation between the stop-band frequency and λ_0 for the chosen parameters. However, we will show in the following that such condition can also be obtained in this case.

In the electrostatic limit, we can obtain g, Δ_1, Δ_2 when $\epsilon_2 = \epsilon_3$ as:

$$g^2 = 2q_1q_2 - q_1^2 = q_1^2 \left(2\frac{E_{F1}}{E_{F2}} - 1 \right), \quad (122a)$$

$$\Delta_1 = \frac{q_2}{\sqrt{2q_1q_2 - q_1^2}} = \frac{E_{F1}}{\sqrt{2E_{F1}E_{F2} - E_{F2}^2}}, \quad (122b)$$

$$\Delta_2 = \frac{i(q_2 - q_1)}{\sqrt{2q_1q_2 - q_1^2}} = \frac{i(E_{F1} - E_{F2})}{\sqrt{2E_{F1}E_{F2} - E_{F2}^2}}, \quad (122c)$$

with q_i obtained using $E_F = E_{Fi}$ with $i = 1, 2$ in Eq. (107).

In the electrostatic limit the functions Δ_i will not depend on the plasmon frequency and $g = q_1\sqrt{F'}$, with $F' = 2E_{F1}/E_{F2} - 1$. As we discussed in the previous section, we can also find the condition for the phase matching $\theta_1 = \theta_2$:

$$\sqrt{F'}d_1 = d_2, \quad (123)$$

and so we can engineer a stop-band for any given frequency adjusting d_1, d_2 . Also, as discussed in the previous subsection, the spectra for $\omega \rightarrow \infty$ will become periodic with respect to $q \propto \omega^2$, a result that comes from the parameters Δ_i becoming frequency independent.

In Fig. 8 we show the reflectance as function of $E_{F2} - 2E_{F1}$ and the plasmon frequency. When $E_{F2} - 2E_{F1} > 0$, we have that g^2 , given by Eq. (122a), is negative, implying evanescence transport and explaining the large bright area with $\mathcal{R} = 1$.

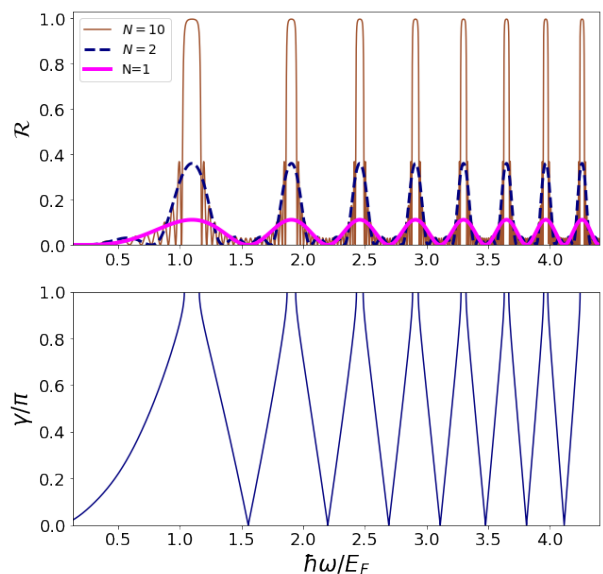


Figure 5. Top panel: Reflectance of a graphene SPP from a Bragg grating with lengths $1L$, $2L$, and $10L$. The dielectrics constants are $\epsilon_1 = \epsilon_3 = 1$ and $\epsilon_2 = 2$. Also we have $E_{F1} = E_{F2} = 0.5 \text{ eV}$. We have fixed the wavelength of the plasmon λ_0 for the frequency $\hbar\omega_0 = 1.1E_{F1}$ and we used $h = \lambda_0$, $d_1 = \lambda_0/(4\sqrt{F})$, and $d_2 = \lambda_0/4$, with F given by Eq. (120). This choice makes $\theta_1 = \theta_2$. We can see a gap opening at the frequency $1.1E_{F1}/\hbar$. Bottom panel: The respective dispersion relation of the plasmonic crystal.

For $E_{F2} \rightarrow 0$, we have that $g/q_1 \rightarrow \infty$, meaning that the wavelength in the region with σ_2 will be significantly smaller than the wavelength of the incoming plasmon, making the system acting as a Fabry-Pèrot cavity, explaining the large number of fringes around $E_{F2} - 2E_{F1} \approx -0.5 \text{ eV}$, that is, when $E_{F2} \approx 0$. When $E_{F2} \approx E_{F1}$, that happens for $E_{F2} - 2E_{F1} = -0.26 \text{ eV}$ the reflectance goes to zero, as expected. We can also see that in respect to the difference $\Delta E_F = E_{F2} - E_{F1}$ the reflectance is asymmetric. This also happens for an electron scattering through a square well: the reflectance have different behavior if the square well is positive or negative.

VIII. CONCLUSIONS

We have used coupled-mode and transfer matrix theory for describing the scattering of a metallic SPP and a graphene SPP from a square-wave Bragg grating written on the interface between a metal and a dielectric and between two different dielectrics, respectively. The method allows for simple analytical expressions for the reflectance coefficient \mathcal{R} and the dispersion relation of the Bragg grating. Our results are valid within the approximations that the coupling of the SPP mode to radiation and evanescent modes is small. Relaxing this approximation is possible, but analytical results are no longer

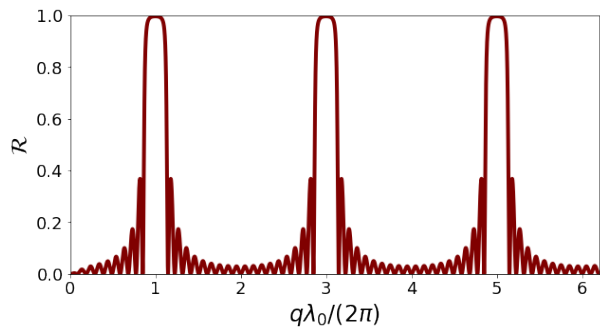


Figure 6. Periodicity of the reflection as function of the wavenumber q using the same parameters of Fig. (5). The periodicity is a consequence of the phase matching $\theta_1 = \theta_2$ between the two different cells of the Bragg grating. The stopbands appears when $q\lambda_0 = 2\pi(1 + 2n)$, with n an integer.

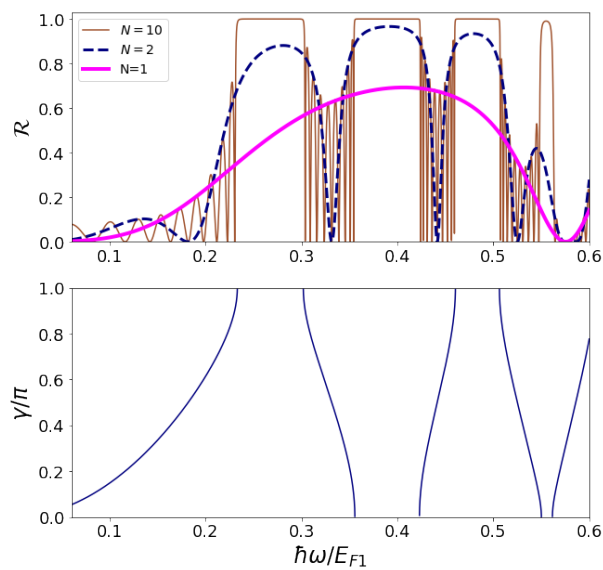


Figure 7. Reflectance of a graphene SPP from a Bragg grating with $N = 10$ unit cells. Parameters: $\epsilon_1 = 1$, $\epsilon_2 = \epsilon_3 = 4$, $E_{F1} = 0.3$ eV, $E_{F2} = 0.55$ eV, λ_0 is the wavelength for a frequency of $\hbar\omega = E_{F1}/2$ and we fixed $d_1 = d_2 = \lambda_0/2$. In the bottom panel we have the dispersion relation for the plasmonic crystal.

available.

We used the analytical results to study the reflection and dispersion relation for different plasmonic Bragg gratings. We characterized the condition to have sinusoidal or evanescent transport. For a Bragg grating consisting of alternating metals with different plasmonic frequencies, we show that there will be an infinite number of bands when the grating metal has a lower plasmonic frequency than the substrate metal.

We have also shown that the transfer matrix parameters for graphene SPPs are frequency independent in the electrostatic limit. With this result, we could find the condition for phase matching of the traveling wave inside

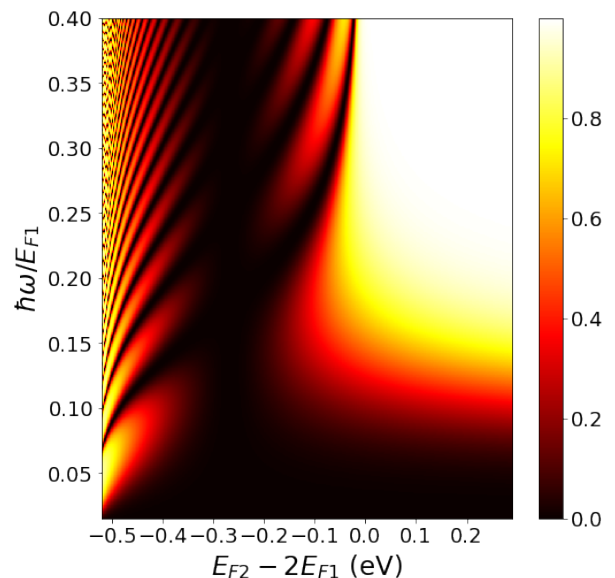


Figure 8. Reflectance of a graphene SPP from a single unit cell as function of the difference in the Fermi energy and incoming SPP frequency. The bright region that appears when $E_{F2} - 2E_{F1} > 0$ is a consequence of the evanescent transport along the graphene strips in the σ_2 region. The parameters are chosen as: $\epsilon_1 = 1$, $\epsilon_2 = \epsilon_3 = 4$, $E_{F1} = 0.26$ eV. λ_0 is the wavelength for a plasmon frequency of $0.2E_{F1}/\hbar$ and $d_1 = d_2/2 = \lambda_0/4$.

each component of the Bragg grating, finding the condition for engineering a stop-band for any given frequency.

ACKNOWLEDGMENTS

N.M.R.P. acknowledges Bruno Amorim for discussions in the early stage of the this work. N.M.R.P. acknowledges support from the European Commission through the project ‘‘Graphene-Driven Revolutions in ICT and Beyond’’ (Ref. No. 785219), COMPETE2020, PORTUGAL2020, FEDER and the Portuguese Foundation for Science and Technology (FCT) through project POCI-01-0145-FEDER-028114 and in the framework of the Strategic Financing UID/FIS/04650/2013.

Appendix A: Lorentz reciprocity theorem

We pause here for a moment for deriving a useful theorem. The employed technique will prove useful in the next section. The complex time-averaged Poyting vector of the mode ν (here including the z -dependence) is given by

$$S_{\nu,z} = \frac{1}{2} \Re(\mathbf{E}_\nu \times \mathbf{H}_\nu^*) \cdot \mathbf{e}_z. \quad (\text{A1})$$

Let \mathbf{E}_ν , \mathbf{H}_ν and \mathbf{E}_μ , \mathbf{H}_μ be two modes of Maxwell’s equations with $\epsilon(x, z) = \epsilon(x)$, including

the z -dependence (even if it is only a trivial phase). Maxwell's equations for the mode read (in this case we assume that the β -dependence is included in the mode, as we have not made explicit the transverse component of the field)

$$\nabla \times \mathbf{H}_\nu = -i\omega\epsilon_0\epsilon\mathbf{E}_\nu, \quad (\text{A2})$$

$$\nabla \times \mathbf{E}_\nu = i\omega\mu_0\mathbf{H}_\nu, \quad (\text{A3})$$

and equivalent equations for \mathbf{E}_μ and \mathbf{H}_μ . Taking the dot product to the left of the first previous equation with \mathbf{E}_μ it follows that

$$\mathbf{E}_\mu \cdot \nabla \times \mathbf{H}_\nu = -i\omega\epsilon_0\epsilon\mathbf{E}_\mu \cdot \mathbf{E}_\nu, \quad (\text{A4})$$

and taking the dot product of Eq. (A3) with \mathbf{H}_μ it follows that

$$\mathbf{H}_\mu \cdot \nabla \times \mathbf{E}_\nu = i\omega\mu_0\mathbf{H}_\mu \cdot \mathbf{H}_\nu \quad (\text{A5})$$

Adding of the two previous equations we obtain

$$\begin{aligned} \mathbf{E}_\mu \cdot (\nabla \times \mathbf{H}_\nu) + \mathbf{H}_\mu \cdot (\nabla \times \mathbf{E}_\nu) = \\ -i\omega\epsilon_0\epsilon\mathbf{E}_\mu \cdot \mathbf{E}_\nu + i\omega\mu_0\mathbf{H}_\mu \cdot \mathbf{H}_\nu. \end{aligned} \quad (\text{A6})$$

Next, we use the identity (A and B two vector fields)

$$\nabla \cdot (\mathbf{A} \times \mathbf{B}) = -\mathbf{A} \cdot (\nabla \times \mathbf{B}) + \mathbf{B} \cdot (\nabla \times \mathbf{A}), \quad (\text{A7})$$

which leads to

$$\begin{aligned} -\nabla \cdot (\mathbf{E}_\mu \times \mathbf{H}_\nu) + \mathbf{H}_\nu \cdot (\nabla \times \mathbf{E}_\mu) \\ + [-\nabla \cdot (\mathbf{H}_\mu \times \mathbf{E}_\nu) + \mathbf{E}_\nu \cdot (\nabla \times \mathbf{H}_\mu)] = \\ = -i\omega\epsilon_0\epsilon\mathbf{E}_\mu \cdot \mathbf{E}_\nu + i\omega\mu_0\mathbf{H}_\mu \cdot \mathbf{H}_\nu, \end{aligned} \quad (\text{A8})$$

which simplifies (after using Maxwell's equations) to

$$\nabla \cdot (\mathbf{E}_\mu \times \mathbf{H}_\nu - \mathbf{E}_\nu \times \mathbf{H}_\mu) = 0, \quad (\text{A9})$$

a relation known as Lorentz reciprocity theorem. Again, we separate the operator ∇ in its transverse and longitudinal, as in Eq. (7). Also we recall the dependence of the modes in the coordinate z : $\mathbf{E}_\mu = \mathcal{E}_\mu e^{i\beta z}$ and the same for \mathbf{H}_μ . With this, Eq. (A9) transforms into

$$\begin{aligned} \nabla_t \cdot (\mathcal{E}_\mu \times \mathcal{H}_\nu - \mathcal{E}_\nu \times \mathcal{H}_\mu)_t \\ + i(\beta_\nu + \beta_\mu)\mathbf{e}_z \cdot (\mathcal{E}_{\mu,t} \times \mathcal{H}_{\nu,t} - \mathcal{E}_{\nu,t} \times \mathcal{H}_{\mu,t})_z = 0 \end{aligned} \quad (\text{A10})$$

Next, we integrate the previous equation in the transversal direction to the waveguide, leading to

$$\begin{aligned} \mathbf{e}_x \cdot \int dx \frac{\partial}{\partial x} (\mathcal{E}_\mu \times \mathcal{H}_\nu - \mathcal{E}_\nu \times \mathcal{H}_\mu)_t = \\ -i(\beta_\nu + \beta_\mu) \int dx \mathbf{e}_z \cdot (\mathcal{E}_{\mu,t} \times \mathcal{H}_{\nu,t} - \mathcal{E}_{\nu,t} \times \mathcal{H}_{\mu,t}). \end{aligned} \quad (\text{A11})$$

The integral on the LHS is elementary and it gives zero, since the fields vanish at infinity. It follows that

$$(\beta_\nu + \beta_\mu) \int dx \mathbf{e}_z \cdot (\mathcal{E}_{\mu,t} \times \mathcal{H}_{\nu,t} - \mathcal{E}_{\nu,t} \times \mathcal{H}_{\mu,t}) = 0, \quad (\text{A12})$$

which is an integral version of Lorentz's reciprocity relation.

Appendix B: Derivation of the orthogonality condition

Let us now use the procedure of the Appendix for deriving the orthogonality relation between the modes. Let us take the dot product of \mathbf{E}_ν with the complex conjugate of Eq. (A2):

$$\mathbf{E}_\nu \cdot \nabla \times \mathbf{H}_\mu^* = i\omega\epsilon_0\epsilon\mathbf{E}_\nu \cdot \mathbf{E}_\mu^*, \quad (\text{B1})$$

and taking the dot product of \mathbf{H}_μ^* with Eq. (A3):

$$\mathbf{H}_\mu^* \cdot \nabla \times \mathbf{E}_\nu = i\omega\mu_0\mathbf{H}_\mu^* \cdot \mathbf{H}_\nu. \quad (\text{B2})$$

Subtracting the two previous equations we obtain

$$\mathbf{E}_\nu \cdot \nabla \times \mathbf{H}_\mu^* - \mathbf{H}_\mu^* \cdot \nabla \times \mathbf{E}_\nu = i\omega\epsilon_0\epsilon\mathbf{E}_\nu \cdot \mathbf{E}_\mu^* - i\omega\mu_0\mathbf{H}_\mu^* \cdot \mathbf{H}_\nu \quad (\text{B3})$$

or

$$\nabla \cdot (\mathbf{E}_\nu \times \mathbf{H}_\mu^*) = -i\omega(\epsilon_0\epsilon\mathbf{E}_\nu \cdot \mathbf{E}_\mu^* - \mu_0\mathbf{H}_\mu^* \cdot \mathbf{H}_\nu). \quad (\text{B4})$$

We now interchange μ and ν in the previous equation and take the complex conjugate:

$$\nabla \cdot (\mathbf{E}_\mu^* \times \mathbf{H}_\nu) = i\omega(\epsilon_0\epsilon\mathbf{E}_\mu^* \cdot \mathbf{E}_\nu - \mu_0\mathbf{H}_\nu \cdot \mathbf{H}_\mu^*), \quad (\text{B5})$$

where we used $\epsilon^* = \epsilon$, that is, we are dealing with a lossless system.

Adding the two previous equations it follows that

$$\nabla \cdot (\mathbf{E}_\nu \times \mathbf{H}_\mu^* + \mathbf{E}_\mu^* \times \mathbf{H}_\nu) = 0. \quad (\text{B6})$$

Let us again separate the ∇ operator in its transverse and longitudinal parts. Recalling the dependence of the modes in the coordinate z we obtain from Eq. (B6):

$$\begin{aligned} \nabla_t \cdot (\mathcal{E}_\nu \times \mathcal{H}_\mu^* + \mathcal{E}_\mu^* \times \mathcal{H}_\nu)_t \\ + i(\beta_\nu - \beta_\mu)\mathbf{e}_z \cdot (\mathcal{E}_{\nu,t} \times \mathcal{H}_{\mu,t}^* - \mathcal{E}_{\mu,t}^* \times \mathcal{H}_{\nu,t}) = 0 \end{aligned} \quad (\text{B7})$$

If we now integrate over the transverse x -direction, considering $\beta_\nu \neq \beta_\mu$, and using the same procedure that led us to Eq. (A12), we obtain Eq. (37) in the main text.

Appendix C: Coupled mode theory with a sheet of graphene

The inclusion of a graphene sheet can be done adding a surface current in Eq. (3):

$$\nabla \times \mathbf{H} = \sigma\delta(z)\mathbf{E}_\parallel - i\omega\epsilon_0\epsilon\mathbf{E}, \quad (\text{C1})$$

or

$$\nabla \times \mathbf{H} = -i\omega\epsilon_0 \left(\epsilon + i\hat{\mathbf{r}}_\parallel \frac{\sigma\delta(x)}{\omega\epsilon_0} \hat{\mathbf{r}}_\parallel \right) \mathbf{E}, \quad (\text{C2})$$

to avoid singularities we substitute the delta function to a function $g_\delta(x)$ with the property $\lim_{\delta \rightarrow 0} g_\delta(x) = \delta(x)$. We can use for example:

$$g_\delta(x) = \frac{1}{\pi} \frac{\delta}{x^2 + \delta^2}. \quad (\text{C3})$$

$$K_{\mu,\nu}(z) = \frac{i\omega\epsilon_0}{4\mathcal{P}} \int dx [\epsilon(x, z) - \epsilon(x)] \mathcal{E}_{\mu,x}^* \mathcal{E}_{\nu,x}, \quad (\text{C4})$$

$$k_{\mu,\nu}(z) = \frac{i\omega\epsilon_0}{4\mathcal{P}} \int dx \frac{\epsilon(x) + i\frac{\sigma g_\delta(z)}{\omega\epsilon_0}}{\epsilon(x, z) + i\frac{\sigma g_\delta(z)}{\omega\epsilon_0}} \left(\epsilon(x, z) + i\frac{\sigma g_\delta(z)}{\omega\epsilon_0} - \epsilon(x) - i\frac{\sigma g_\delta(z)}{\omega\epsilon_0} \right) \mathcal{E}_{\mu,z}^* \mathcal{E}_{\nu,z}, \quad (\text{C5})$$

the coupling constant $K_{\mu,\nu}(z)$ does not change its definition because the tensor only couples the surface current of graphene with the component z of the electric field.

The effective dielectric function $\epsilon + i\hat{\mathbf{r}}_{\parallel} \frac{\sigma\delta(x)}{\omega\epsilon_0} \hat{\mathbf{r}}_{\parallel}$ will be a tensor, however the results of the Sec. III and Appendix A and B can be show to still be valid.

The coupling constants $K_{\mu,\nu}$ and $k_{\mu,\nu}$ using Eqs. (53) and (54) need to be written as:

$$k_{\mu,\nu}(z) = \frac{i\omega\epsilon_0}{4\mathcal{P}} \left[\int_{-\infty}^{-\delta} + \int_{\delta}^{\infty} \right] dx \frac{\epsilon(x)}{\epsilon(x, z)} (\epsilon(x, z) - \epsilon(x)) \mathcal{E}_{\mu,z}^* \mathcal{E}_{\nu,z} + \frac{i\omega\epsilon_0}{4\mathcal{P}} \int_{-\delta}^{\delta} dx (\epsilon(x, z) - \epsilon(x)) \mathcal{E}_{\mu,z}^* \mathcal{E}_{\nu,z}. \quad (\text{C6})$$

however, the last integral of Eq. (C6) is not singular, and so, as we take the limit $\delta \rightarrow 0$, the last integral vanishes and we reobtain Eq. (54).

For $|z| < \delta$, we have that $\epsilon(x, z) + i\frac{\sigma g_\delta(z)}{\omega\epsilon_0} \approx i\frac{\sigma g_\delta(z)}{\omega\epsilon_0}$. For $z > \delta$ we have that $g_\delta(z) \approx 0$. So Eq. (C5) can be written as:

$$K_{\mu,\nu}(z) = \frac{i\omega\epsilon_0}{4\mathcal{P}} \int dx [\epsilon(x, z) - \epsilon(x)] \mathcal{E}_{\mu,x}^* \mathcal{E}_{\nu,x}, \quad (\text{C7})$$

$$k_{\mu,\nu}(z) = \frac{i\omega\epsilon_0}{4\mathcal{P}} \int dx \frac{\epsilon(x) + i\frac{\sigma_1 g_\delta(x)}{\omega\epsilon_0}}{\epsilon(x, z) + i\frac{\sigma_2(z) g_\delta(x)}{\omega\epsilon_0}} \left(\epsilon(x, z) + i\frac{\sigma_2(z) g_\delta(x)}{\omega\epsilon_0} - \epsilon(x) - i\frac{\sigma_1 g_\delta(x)}{\omega\epsilon_0} \right) \mathcal{E}_{\mu,z}^* \mathcal{E}_{\nu,z}, \quad (\text{C8})$$

after simplifying and taking the limit $\delta \rightarrow 0$:

$$K_{\mu,\nu}(z) = \frac{i\omega\epsilon_0}{4\mathcal{P}} \int dx [\epsilon(x, z) - \epsilon(x)] \mathcal{E}_{\mu,x}^* \mathcal{E}_{\nu,x}, \quad (\text{C9})$$

$$k_{\mu,\nu}(z) = -\frac{\sigma_1}{\sigma_2(z)} \frac{[\sigma_2(z) - \sigma_1]}{4\mathcal{P}} \mathcal{E}_{\mu,z}^*(0) \mathcal{E}_{\nu,z}(0) + \frac{i\omega\epsilon_0}{4\mathcal{P}} \int dx \frac{\epsilon(x)}{\epsilon(x, z)} (\epsilon(x, z) - \epsilon(x)) \mathcal{E}_{\mu,z}^* \mathcal{E}_{\nu,z}. \quad (\text{C10})$$

¹ L. Feng, Y.-L. Xu, W. S. Fegadolli, M.-H. Lu, J. E. B. Oliveira, V. R. Almeida, Y.-F. Chen, and A. Scherer, *Experimental demonstration of a unidirectional reflectionless parity-time metamaterial at optical frequencies*, Nat. Matt. **12**, 108 (2013).

² W.-P. Huang, *Coupled-mode theory for optical waveguides: and overview*, J. Opt. Soc. Am. A **11**, 963 (1994).

³ Z. Lin, H. Ramezani, T. Eichelkraut, T. Kottos, H. Cao, and D. N. Christodoulides, *Unidirectional Invisibility Induced by PT-Symmetric Periodic Structures*, Phys. Rev. Lett. **106**, 213901 (2011).

⁴ A. Yariv, *Coupled-Mode Theory for Guided-Wave Optics*, IEEE Journal of Quantum Electronics **QE-9**, 919 (1973).

⁵ H. F. Taylor and A. Yariv, *Guided Wave Optics*, Proceedings of the the IEEE **62**, 1044 (1974).

⁶ P. Yeh, A. Yariv, and C.-S. Hong, *Electromagnetic propagation in periodic stratified media. I. General theory*, J. Opt. Soc. Am. **67**, 423 (1977).

⁷ T. Makino, *Threshold condition of DFB semiconductor lasers by the local-normal-mode transfer-matrix method: correspondence to the coupled-Wave Method*, J. Lightwave Technology **12**, 2092 (1994).

- ⁸ O. Dietz, G. Kewes, O. Neitzke, and O. Benson, *Coupled-mode approach to square-gradient Bragg-reflection resonances in corrugated dielectric waveguides*, Phys. Rev. A **92**, 043834 (2015).
- ⁹ Y. Lou, H. Pan, T. Zhu, and Z. Ruan, *Spatial coupled-mode theory for surface plasmon polariton excitation at metallic gratings*, J. Opt. Soc. Am. **33**, 819 (2016).
- ¹⁰ Z. Ruan, H. Wu, M. Qiu, and S. Fan, *Spatial control of surface plasmon polariton excitation at a planar metal surface*, Opt. Lett. **39**, 3587 (2014).
- ¹¹ Z. Chen, R. Zhoua, L. Wua, S. Yang, and D. Liu, *Surface plasmon characteristics based on graphene-cavity-coupled T waveguide system*, Sol. Stat. Comm. **28**, 50 (2018).
- ¹² L.-H. Hong, B.-Q. Chen, C.-Y. Hu, and Z.-Y. Li, *Analytical solution of second-harmonic generation in a lithium-niobate-birefringence thin-film waveguide via modal phase matching*, Phys. Rev. A **98**, 023820 (2018).
- ¹³ J. Petracek and V. Kuzmiak, *Transverse Anderson localization of channel plasmon polaritons*, Phys. Rev. A **98**, 023806 (2018).
- ¹⁴ P. Graczyk and M. Krawczyk, *Coupled-mode theory for the interaction between acoustic waves and spin waves in magnonic-phononic crystals: Propagating magnetoelastic waves*, Phys. Rev. B **96**, 024407 (2017).
- ¹⁵ E. Santamato and P. Maddalena, *Coupled-mode theory for nonlinear interaction of surface plasmons/polaritons*, II Nuovo Cimento **70**, 268 (1982).
- ¹⁶ E. A. Ostrovskaya, Y. S. Kivshar, M. Lisak, B. Hall, F. Cattani, and D. Anderson, *Coupled-mode theory for Bose-Einstein condensates*, Phys. Rev. A **61**, 031601(R) (2000).
- ¹⁷ G. Sun, J. B. Khurgin, and A. Bratkovsky, *Coupled-mode theory of field enhancement in complex metal nanostructures*, Phys. Rev. B **84**, 045415 (2011).
- ¹⁸ P. Pelet and N. Engheta, *Coupled-mode theory for chiro-waveguides*, J. Appl. Phys. **67**, 2742 (1990).
- ¹⁹ Yu. V. Bludov, N. M. R. Peres, G. Smirnov, M. I. Vasilevskiy, *Scattering of surface plasmon-polaritons in a graphene multilayer photonic crystal with inhomogeneous doping*, Phys. Rev. B **93**, 245425 (2016).
- ²⁰ A. J. Chaves, B. Amorim, Yu. V. Bludov, P. A. D. Gonçalves, N. M. R. Peres, *Scattering of graphene plasmons at abrupt interfaces: an analytic and numeric study*, Phys. Rev. B **97**, 035434 (2018).
- ²¹ D. Marcuse, *Theory of Optical Dielectric Waveguides*, Chap. 3, (Academic Press, New York, 1974).
- ²² H. Kogelnik, *Theory of Dielectric Waveguides*, in *Integrated Optics*, edited by T. Tamir, Chap.2, (Springer, Berlin, 1975).
- ²³ C. R. Pollock and M. Lipson, *Integrated Photonics*, Chap. 10, (Springer, New York, 2003).
- ²⁴ A. Yariv and P. Yeh, *Optical Waves in Crystal*, Chap. 6, (Wiley, USA, 1984).
- ²⁵ H. A. Haus, and W. Huang, *Coupled-mode theory*, Proceedings of the the IEEE, **79**, 1505 (1991).
- ²⁶ A. W. Snyder and J. D. Love, *Optical Waveguide Theory*, Chap. 27, (Chapman and Hall, New York, 1983).
- ²⁷ D. Marcuse, *Light Transmission Optics*, Chap. 8, (VNR, New York, 1982).
- ²⁸ P. A. D. Gonçalves and N. M. R. Peres, *An Introduction to Graphene Plasmonics*, (Word Scientific, Singapore, 2016).
- ²⁹ M. Peter and C. M. Soukoulis, *Wave propagation: from electrons to photonic crystals and left-handed materials*, (Princeton University Press, 2008).